A standardized and automated method of perineuronal net analysis using *Wisteria floribunda* agglutinin staining intensity

Megan L. Slaker, John H. Harkness, Barbara A. Sorg[*]

Department of Integrative Physiology and Neuroscience, Washington State University, Vancouver, WA 98686, USA

ARTICLE INFO

ABSTRACT

Perineuronal nets (PNNs) are aggregations of extracellular matrix molecules that are critical for plasticity. Their altered development or changes during adulthood appear to contribute to a wide range of diseases/disorders of the brain. An increasing number of studies examining the contribution of PNN to various behaviors and types of plasticity have analyzed the fluorescence intensity of *Wisteria floribunda* agglutinin (WFA) as an indirect measure of the maturity of PNNs, with brighter WFA staining corresponding to a more mature PNN and dim WFA staining corresponding to an immature PNN. However, a clearly-defined and unified method for assessing the intensity of PNNs is critical to allow us to make comparisons across studies and to advance our understanding of how PNN plasticity contributes to normal brain function and brain disease states. Here we examined methods of PNN intensity quantification and demonstrate that creating a region of interest around each PNN and subtracting appropriate background is a viable method for PNN intensity quantification that can be automated. This method produces less variability and bias across experiments compared to other published analyses, and this method increases reproducibility and reliability of PNN intensity measures, which is critical for comparisons across studies in this emerging field.

1. Introduction

Perineuronal nets (PNNs) are unique aggregations of extracellular matrix (ECM) that surround a subset of neurons in the brain and are commonly labeled with the plant lectin *Wisteria floribunda* agglutinin (WFA); (Hartig et al., 1992). Recently, there has there been intense focus on the role of PNNs in normal brain function, such as critical period development and learning and memory, and in many disorders or pathologies, such as recovery from nerve damage, schizophrenia, Alzheimer's disease, stroke, epilepsy, fear memory, and drug addiction (Pizzorusso et al., 2002; Galtrey et al., 2007; Fawcett, 2009; Gogolla et al., 2009; Mauney et al., 2013; Xue et al., 2014; Slaker et al., 2015; Yang et al., 2015; Yutsudo and Kitagawa, 2015). The reason for this focus on PNNs in recent years is the centralizing and exciting concept that PNNs *limit plasticity* in adulthood and that they can be degraded to *reinstate* juvenile-like states of plasticity to produce axon sprouting and regeneration of function in damaged neurons. As such, PNNs play key roles in neural development, synaptogenesis, neuroprotection, and experience-dependent synaptic plasticity (Celio et al., 1998; Dityatev and Schachner, 2003; McRae and Porter, 2012; Soleman et al., 2013; Suttkus et al., 2016).

An increasing number of studies examining the contribution of PNNs to various behaviors and types of plasticity have analyzed the fluorescence intensity of WFA as an indirect measure of the maturity of PNNs — with mature PNNs labeled with more intense WFA stain and immature PNNs labeled with less intense WFA stain (Foscarin et al., 2011; Cabungcal et al., 2013a, 2013b; Carulli et al., 2013; Happel et al., 2014; Chen et al., 2015; Slaker et al., 2015; Vazquez-Sanroman et al., 2015a; 2015b). While WFA intensity is important for formulating experiments and interpreting the findings, the method by which WFA intensity is measured and analyzed has been *inconsistent* across studies. Some studies have used semi-

---

quantitative methods to examine relative intensity changes, but these studies lack measures of *individual* PNNs (Wang et al., 2011; Deak et al., 2012; Yamada and Jinno, 2013; Racz et al., 2014; Kecskes et al., 2015). Other studies examine changes in individual PNNs by averaging the intensity of 15 pixels within a given PNN around the soma (Foscarin et al., 2011; Carulli et al., 2013; Vazquez-Sanroman et al., 2015a), and others have not included details in the methodology (Chen et al., 2015). The diversity of analyses within this relatively young, but rapidly growing area of study makes it difficult to compare analyses across studies that have identified important changes in PNN staining intensity. Here, we provide evidence that creating a region of interest (ROI) surrounding each PNN within a field and conducting adequate background subtraction is a reproducible and consistent method to measure WFA staining intensity. Additionally, this method has been automated, which can increase the speed of analysis by 100-fold.

1.1. Experimental procedures

1.1.1. Animals

A total of 8 male Sprague-Dawley rats (280–300 g) were obtained from Simonsen Laboratories (Gilroy, CA) and were singly housed in a temperature- and humidity-controlled room with a 12 h light/dark cycle with lights on at 07:00 with food and water *ad libitum.* All experiments were conducted according to the National Institutes of Health *Guide for the Care and Use of Laboratory Animals* (NIH Publications No. 80-23) and were approved by the Institutional Animal Care and Use Committee. All efforts were made to minimize pain and suffering. Rats were perfused intracardially with 4% paraformaldehyde (PFA) in 1X-PBS. The brains were removed and stored overnight in 4% PFA at 4 °C. The next day, brains were moved to a 20% sucrose solution and 24 h later were flash frozen at −80 °C and stored until WFA staining.

1.1.2. Histology and WFA staining

Coronal brain sections through the prefrontal cortex (PFC; +4.0 through +3.6 from bregma; Paxinos and Watson, 2007) and dorsal hippocampus (−2.0 through −4.0 from bregma; Paxinos and Watson, 2007) were cut at 30 μm using a freezing microtome. WFA staining was performed by washing free-floating sections three times for 5 min in 1X-PBS, the tissue was placed in 3% goat blocking serum (Vector Laboratories) for 1 h and was then incubated overnight at 4 °C on a shaker table with fluorescein-conjugated WFA (1:500, Vector Laboratories) in 1X-PBS containing 2% goat serum. The tissue was washed three times for 10 min each time in 1X-PBS and mounted onto Frost plus slides in diluted 1X-PBS (30:200) with 0.24% Triton X-100 (Sigma-Aldrich). After drying, ProLong (Life Technologies) was applied followed by a coverslip and allowed to dry at least 3 days at 4 °C.

1.1.3. Imaging

Tissue was imaged using a Leica SP8 laser scanning confocal microscope with an HCX PL apo CS, dry, 20× objective with 0.70 numerical aperture. The 488 nm laser was used for excitation and a photomultiplier tube detected emission photons within the range of 495–545 nm. Leica Application Suite was used for image acquisition. Laser intensity, gain, offset, and pinhole settings were determined by setting the limits to include sub-saturated pixels and true-black pixels within a section of the orbitofrontal cortex (OF) from one rat. The OF was chosen because we have found there to be the greatest range of WFA staining of PNNs in this region. These settings were kept constant for all images. Images were taken through a z-plane (8.5 μm) within the center of the tissue section, containing 20 stacks (0.4 μm/stack) from the prelimbic PFC (PL), OF, dorsal hippocampus (Hip), and caudate/putamen (CPu). These

regions were selected to examine differences in methodology based on the intensity of PNNs. Since PNNs are located surrounding the outside of neurons, it is important to image through a z-stack to provide a more complete image of the PNNs. Imaging in one plane can bias and restrict the data that can be obtained. Once all images were acquired, raw data were exported as 8-bit, grayscale, tiff files. Raw, 8-bit data allows for collection of a dynamic range from 0 to 255 arbitrary unites (au) for each pixel intensity value, whereas data exported as RBG limits the dynamic range from 0 to 85 (au). The z-stack was then projected into a sum slices image using ImageJ (NIH) software. This method of image projection maintains all data obtained from the z stack and allows the image to be analyzed in two dimensions.

1.1.4. WFA quantification

ImageJ (NIH) software was used for all quantification. The sum of slices projection was used to provide a representation of the intensity values across all images in the z-stack. We examined 8–15 sum-slice images from each brain area to compare three methods of quantification: "Point", "ROI", and PIPSQUEAK; the latter is the automated version of "ROI" (see below). The Point method has been used in previous studies (Foscarin et al., 2011; Carulli et al., 2013; Vazquez-Sanroman et al., 2015a). For the Point method, an experimenter blind to the treatment conditions randomly selected 15 points (pixels) within a PNN. Since the shape of the PNN varies, only points surrounding somata were selected so that they are relatively consistent across the shapes (ignoring the proximal dendrites which are also typically surrounded by PNNs). The intensity of these 15 points was then averaged to represent the average intensity of the individual PNN. Previous studies using this method have not provided extensive detail regarding how background values were determined. For the present study, a background intensity value, taken from one pixel near the PNN, was subtracted from the average. For the ROI method, the background staining was removed from each image with two steps. First, the Rolling Ball Radius function, which removes smooth continuous background, on ImageJ was used to remove variability in background staining across the image (algorithm inspired by Sternberg (Sternberg, 1983)). Second, an ROI was created within four regions of an image lacking a PNN, and the average intensity and SD of each of these ROIs were determined using ImageJ. The ROI with the higher value was selected to represent the background. The background was set to 2 SD above the average in this ROI as the threshold of the image to separate PNN staining from general ("loose") ECM staining. All pixels below this threshold were set to NaN ("not a number"; i.e., not counted as a pixel). ROIs were created surrounding each PNN within the image, including the proximal dendrites. An ROI was created if the PNN surrounding the soma encircled at least 2/3 of the soma. The average intensity for each PNN was calculated and recorded.

Automated analysis of PNN intensity was developed as a macro plugin, called "Perineuronal net Intensity Program for the Standardization and Quantification of ECM Analysis" (PIPSQUEAK), for use with FIJI (FIJI Is Just ImageJ) software. The macro follows the ROI protocol described above for quantification of single-labeled WFA images. Following background removal with Rolling Ball Radius, identification of PNN structures was based on meeting a minimum limit of above-threshold area within parameters of shape requirements. Background subtraction was conducted as described above for ROI, with the exception that 20 ROI sections were selected around the perimeter of the image, high and low outlier ROIs were removed, and those remaining were used for calculation of mean background. All PNN identification parameters are changeable within the program to be able to better match size and shape within different brain areas, thus allowing for exclusion of labeling

that does not meet threshold requirements for size and intensity. ROIs were then constructed around the WFA labels and intensity was measured. The PIPSQUEAK program can also be run in semi-autonomous mode (see Discussion), providing the chance for user review of identified cells. For the Hip and CPu, analysis by PIP-SQUEAK was done in "semi-autonomous mode" because of the greater amount of white matter in these areas. To test the performance of PIPSQUEAK without user influence, analysis of WFA
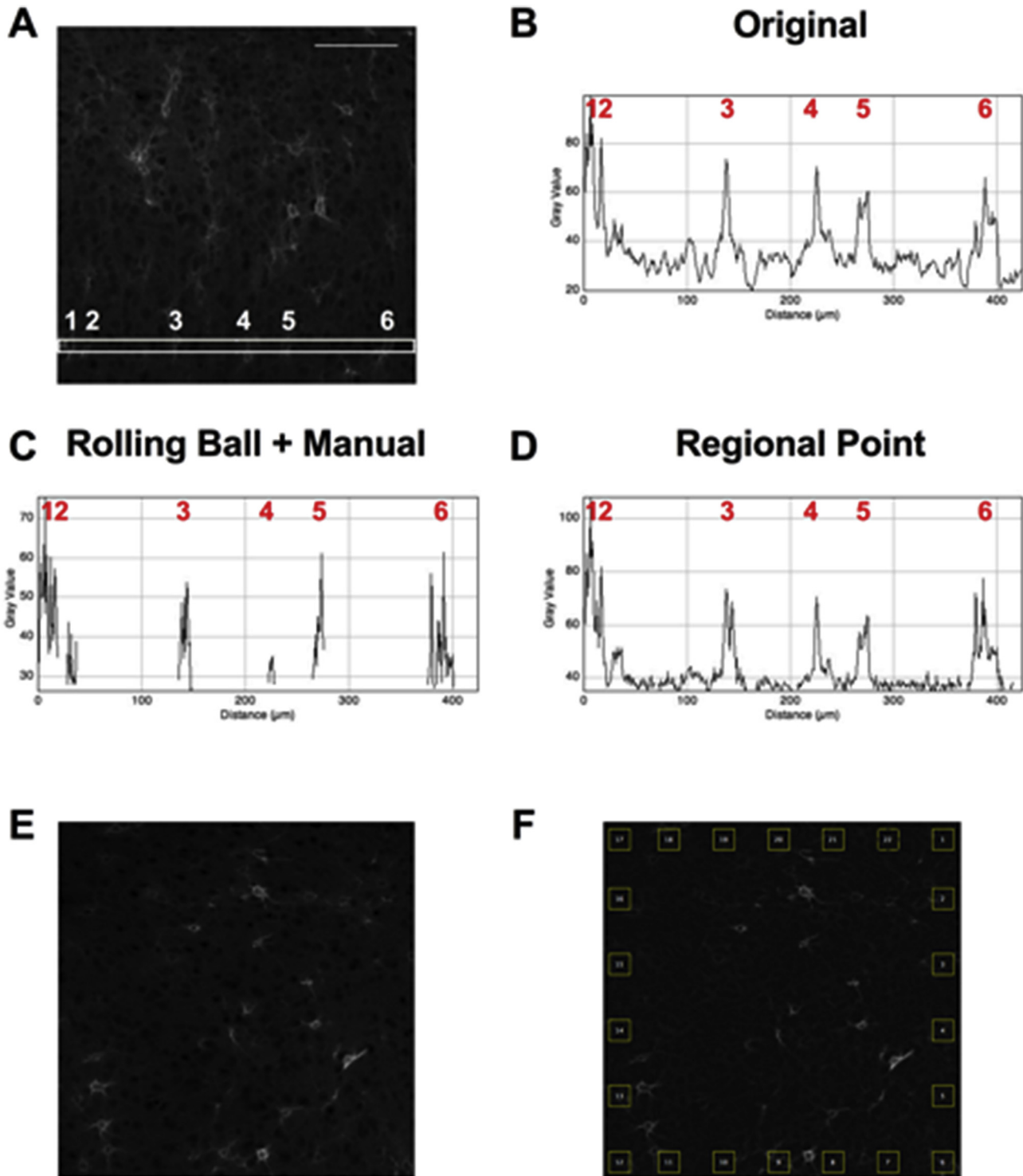

Fig. 1. Background subtraction method alters pixels included in assessment and pixel values. **A)** Representative image from the PFC. Box indicates region analyzed with the plot profiles. Numbers correspond to portions of PNNs included in the box. White scale bar represents 100 μm. **B)** Original plot profile from the box in A. PNN peaks are identified with numbers corresponding to the numbers in A. **C)** Plot profile following the Rolling Ball Radius function and manual background subtraction. The gaps in the trace indicate pixels below the background level. **D)** Plot profile following selection of one point from a region adjacent to each PNN as the background. **E)** Summed image without background subtraction prior to PIPSQUEAK analysis. **F)** Same image as (E) after Rolling Ball Radius background subtraction. Yellow squares are 20 ROI sections selected around the perimeter of the image for calculation of mean background. All gray values are listed in arbitrary units (au).
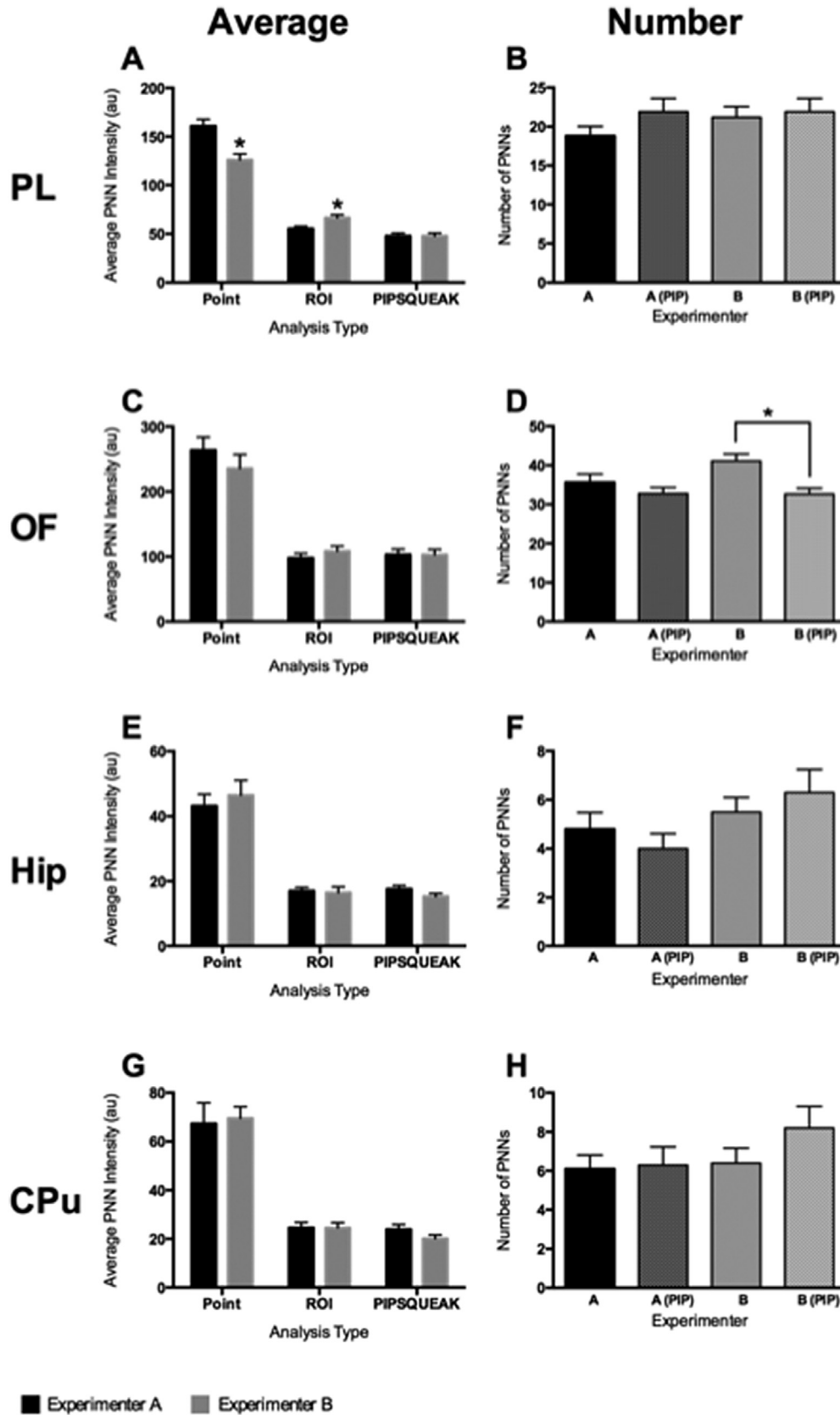
Fig. 2. Effect of quantification method on PNN intensity in different brain regions. Average PNN intensity and number of PNNs from PL PFC, OF PFC, hippocampus, and CPu were analyzed using Point, ROI, and PIPSQUEAK analysis methods by two experimenters (A and B) within the same laboratory to determine the effect of the quantification method on PNN intensities. All PNNs were analyzed within each image. **A)** The average PNN intensity significantly differed between experimenters using the Point and ROI methods, but not different using PIPSQUEAK within the PL region. **B)** There was no significant difference between experimenters in the number of PNNs identified in the PL region. **C)** There were no significant differences in the average intensity between methods in the OF region. **D)** However, experimenter B analyzed significantly more PNNs than PIPSQUEAK in the OF region. **E)** There was no significant difference in average intensity or **F)** in the number of PNNs between experimenters in the hippocampus. **G)** Within the CPu, there was also no difference in the average intensity or **H)** number of PNNs between experiments in each method. Note that for the PL and OF, PIPSQUEAK was run in automatic mode; for Hip and CPu, it was run in semi-autonomous mode. *$p < 0.05$ for the difference in average intensity between experimenters **(A)**, or number of PNNs identified between experimenter B and PIPSQUEAK **(D)**.
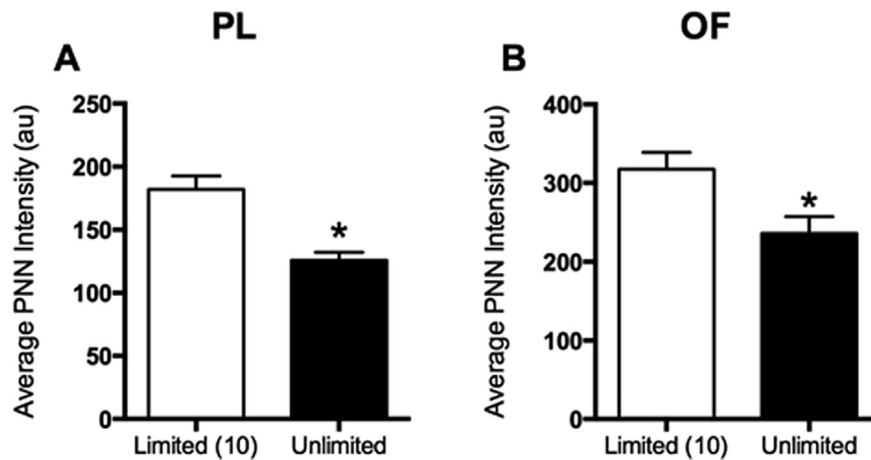
Fig. 3. Comparison of total PNN analysis with analysis limited to 10 PNNs per image within the PL and OF. **A)** Average PNN intensity significantly decreased in the PL region when all PNNs were analyzed compared to a limited PNN number. B) Average PNN intensity also significantly decreased in the OF region when all PNNs were analyzed compared to a limited PNN number. Total number of PNNs average roughly 20 (PL region) and 30 (OF region) per image. $^*p < 0.05$ for the difference in average intensity between limited and unlimited PNN inclusion.

intensity in the PL and OF regions was conducted in "automatic mode". The ImageJ macro and source code are freely available for download at https://labs.wsu.edu/sorg and http://sites.imagej.net/PIPSQUEAK.

1.1.5. Statistics

All statistical tests were conducted using Prism6 software (Graph Pad, Inc.). Unpaired, two-tailed, Student's t-tests were used to examine the difference between experimenters in each analysis type. One-way ANOVAs were used to examine the number of PNNs analyzed across methods. Unpaired, two-tailed, Student's t-tests were used to examine the differences in variation between the ROI and Point methods. Significance was determined by a p value less than 0.05.

2. Results

Background selection can strongly influence the final intensity values for each PNN. Using one image (Fig. 1A), we examined the plot profile (Fig. 1B; histogram of region outlined) after two methods of background subtraction − one used with the ROI method and one used with the Point method. Portions of 6 PNNs are identifiable as peaks within the plot profile (Fig. 1; numbers correspond to PNNs). Within the original image (Fig. 1B), peaks correspond to each PNN and each peak has a different height, indicating differences in maximum intensity. Peak heights range from 48 au (PNN 2) to 100 au (PNN 1). Removing background eliminates values of pixels below that level from analysis. Using the Rolling Ball Radius followed by a manual determination of background (Rolling Ball + Manual), gaps appear between PNNs and the peak heights (ranging from 35 to 75 au) are adjusted based on the background threshold (Fig. 1C). Using one point from a region near each PNN as the background (Regional Point), no visible pixels are missing from the plot profile, indicating that the majority of pixels are above the background (Fig. 1D). Peak heights are also adjusted based on this background, ranging from 50 to 110 au. These results suggest that based on the method of background subtraction, the intensity values can vary greatly and that using the Rolling Ball + Manual background selection provides a more conservative measure of background compared with the Regional Point method. Fig. 1E shows a representative summed image prior to PIPSQUEAK analysis, and Fig. 1F shows the same image following Rolling Ball background subtraction with background ROIs selected.

Next, we sought to determine the effect of the quantification method on PNN intensities (Point, ROI, and PIPSQUEAK). All PNNs were analyzed within each image. The average PNN intensity and number of PNNs from four brain areas were analyzed using all three analysis types by two experimenters (A and B) within the same laboratory. The average PNN intensity was different between experimenters using the Point and ROI methods, but not different using PIPSQUEAK (in automatic mode) within the PL region (Fig. 2A, Student's t-test: Point, $p < 0.001$; ROI, $p < 0.01$; PIPSQUEAK, $p = 1$). The number of PNNs analyzed was not different between experimenters (Fig. 2B, one-way ANOVA, $p = 0.44$).

Within the OF region, experimenter B analyzed more PNNs than the automated methods (Fig. 2D, one-way ANOVA, $p < 0.05$, Sidak's post-hoc test, B vs. B (PIP), $p < 0.005$; B vs. A (PIP), $p < 0.01$). However, there were no differences in the average intensity for any of the methods (Fig. 2C, Student's t-test: Point, $p = 0.35$; ROI, $p = 0.34$; PIPSQUEAK, automatic mode, $p = 0.99$).

Within the Hip, there was no difference in the number (Fig. 2F, one-way ANOVA, $p = 0.16$) or average intensity of PNNs between experimenters (Fig. 2E, Student's t-test: Point, $p = 0.58$; ROI, $p = 0.79$; PIPSQUEAK, $p = 0.13$). Within the CPu, there was no difference in the number (Fig. 2H, one-way ANOVA, $p = 0.32$) or average intensity between experiments in each method (Fig. 2G, Student's t-test: Point, $p = 0.82$; ROI, $p = 0.98$; PIPSQUEAK, $p = 0.15$). Note that analysis by PIPSQUEAK was done in semi-autonomous mode for the Hip and CPu because of the high white matter content of these regions that can produce confounds in the results.

Previous studies examining PNNs have limited the analysis to a set number of PNNs within each region. To examine the effect this limit has, we compared analysis of all PNNs within the PL and OF to analysis of only 10 PNNs per image. We excluded the Hip and CPu because both regions typically had less than 10 PNNs per image. Within both the PL and OF regions, the average PNN intensity was decreased when all PNNs were analyzed compared to when a limited number of PNNs was analyzed (Fig. 3A and B, Student's t-test: PL, $p < 0.003$; OF, $p < 0.05$). Based on the average number of PNNs analyzed from the PL and OF regions (Fig. 2B and D), about 10–20 PNNs were excluded from analysis with the limited number of PNNs.

Finally, we determined the effect of multiple experimenters examining the same 18 PNNs within the same images from the PL region using different methods of analysis. Six experimenters were
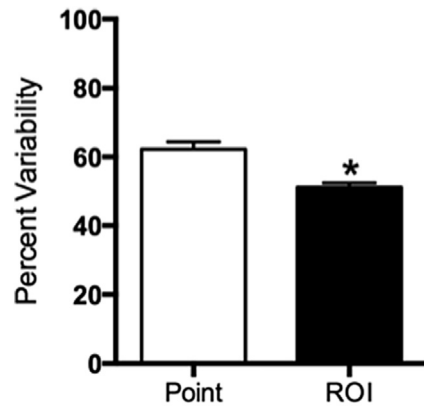
Fig. 4. Variability among experimenters between Point and ROI methods in the PL region. Significantly greater variability was found using the Point method compared to the ROI method among. Six experimenters examining the same PNNs within the same images from the PL region. *$p < 0.05$ for the difference in variability between methods.

used for both of the methods. The coefficient of variance was compared across experimenters within each method to examine the variability. Among the experimenters, greater variability was found using the Point method compared with the ROI method (Fig. 4; Student's t-test, $p < 0.005$).

3. Discussion

In the present study, we demonstrated that for PNN analysis, background subtraction can vary the values for WFA intensity. Furthermore, the ROI method of WFA intensity quantification provides consistent results with lower variance among experimenters compared with the Point method.

Importantly, the Point method also limited the amount of data included in the quantification because it limits the number of PNNs analyzed and the number of pixels included per PNN. The Point method requires an experimenter to randomly identify 15 pixels on each PNN and only on a subset of PNNs within a given field - requiring a conscious decision as to which PNNs and then which pixels within each PNN to include. The PNNs and pixels selected may differ based on the zoom factor of the PNN at the time of analysis, the lighting in the room, the interpretation of the boundary of the PNN, and even the individual's bias of which pixels to measure. While some of these factors can be controlled for, others are much more difficult. These 15 pixels are located around the soma, which overlooks WFA staining located on the proximal dendrites. The ROI method does not have this limitation because it includes all PNNs and pixels within the majority of the PNN in the final analysis. (e.g., soma + proximal dendrites labeled by WFA staining).

One issue to consider is the boundary between the loose ECM and the PNN. For example, what is the level of WFA staining intensity within a PNN vs. the background staining intensity of the loose ECM? This issue could lead to inflated intensity values using the Point method because the experimenter must make a judgment regarding the boundaries of the PNN. The brighter the pixel, the more likely that it is part of a PNN and not the loose ECM. The ROI method does not require the experimenter to make the same judgment regarding the boundary of the PNN, since the ROI includes all pixels within a PNN (potentially those not easily discernable to the human eye). Any background pixels within the ROI method are not included, since they are removed with the Rolling Ball + Manual method of background subtraction. Additionally, an average PNN occupies around 450 μm^2, and therefore using the Point method bases the intensity of that entire area on

less than 5% of the pixels within it. With all of these considerations, the ROI method lessens the likelihood of biasing the intensity values and losing valuable data.

Accurate analysis of PNN histology is essential to determining the effectiveness of treatments on PNNs. Currently, analysis of images captured by confocal microscopy is time intensive, tedious, potentially subjective, and requires expert training. Misidentification of PNN intensity invalidates assumptions reached about treatment efficacy and behavioral correlations. Automation of this process reduces the possibility of unbiased analysis and standardizes analysis across researchers.

Although there is potential for automated PNN identification to misidentify cells or staining not containing PNNs when using PIPSQUEAK, we have taken steps to address this issue. First, the PIPSQUEAK macro is written with the option of being run in a semi-autonomous mode, providing the user an opportunity to audit PNN selection prior to intensity measurement. In regions with high white matter content (Hip and CPu), analysis in the semi-autonomous mode is advantageous to reduce off-target labeling. Secondly, the chance of misidentification is equal across treatment groups, allowing less biased identification of images where intensity is low or high on average—cues that may indicate PNNs are from a particular treatment group even to a researcher blinded to the treatment conditions. In addition, the very high concordance with ROI measurements collected by hand suggests that any contributions by misidentification of neurons will be minimal.

Additionally, our software is capable of processing double-labeled images and labeled cell quantification. While not presented here, we are in the process of validating PIPSQUEAK analysis of double-labeled PNNs. As with single-label analysis, double-label analysis and cell quantification are available in the current release of PIPSQUEAK. Automatic updates to PIPSQUEAK will continue to add features and improve reliability. The addition of double-label analysis continues to improved concordance between automated and human analysis, with a significant possibility that automated analysis will be superior to manual analysis due to heightened specificity and reduced subjectivity.

While not directly tested here, examining the entire population of PNNs decreases the likelihood of identifying a false positive or negative when measuring for changes in PNN intensities. It is possible that the currently used discrete categories of low-, medium-, and high-intensity PNNs relate to different subpopulations of PNN-surrounded neurons (for example, GABAergic vs. glutamatergic), and this can be a useful categorization at present. However, by examining the population as a whole, shifts in the *distribution* of PNN intensities can be observed that are subtler and occur on a continuum across the range of intensities.

While this study focused on WFA staining to measure PNNs, some aggregations of ECM molecules may not be identified using WFA as a marker (Mulligan et al., 1989). Similar methods and considerations should be taken into account when analyzing other markers to quantify intensity of PNNs. It should be noted which marker is analyzed, since WFA labels a distinct population that could differ in intensity compared with other markers, such as aggrecan antibody. Intensity of any of these markers could also be analyzed by PIPSQUEAK.

4. Conclusions

In conclusion, we have demonstrated that the automated ROI method produces results similar to those using the Point method with greater reproducibility and less potential for bias. The current hypothesis in the PNN field is that *increased* WFA intensity corresponds to a mature PNN with decreased capacity for plasticity and that *decreased* WFA intensity corresponds to an immature PNN

with increased capacity for plasticity (Wang and Fawcett, 2012). However, supporting this hypothesis requires a unified method of intensity measurement to advance this emerging field.

Conflicts of interest

The authors declare no conflicts of interest.

References

Cabungcal, J.H., Steullet, P., Kraftsik, R., Cuenod, M., Do, K.Q., 2013a. Early-life insults impair parvalbumin interneurons via oxidative stress: reversal by N-acetylcysteine. Biol. Psychiatry 73, 574–582.

Cabungcal, J.H., Steullet, P., Morishita, H., Kraftsik, R., Cuenod, M., Hensch, T.K., Do, K.Q., 2013b. Perineuronal nets protect fast-spiking interneurons against oxidative stress. Proc. Natl. Acad. Sci. U. S. A. 110, 9130–9135.

Carulli, D., Foscarin, S., Faralli, A., Pajaj, E., Rossi, F., 2013. Modulation of semaphorin3A in perineuronal nets during structural plasticity in the adult cerebellum. Mol. Cell Neurosci. 57, 10–22.

Celio, M.R., Spreafico, R., De Biasi, S., Vitellaro-Zuccarello, L., 1998. Perineuronal nets: past and present. Trends Neurosci. 21, 510–515.

Chen, H., He, D., Lasek, A.W., 2015. Repeated binge drinking increases perineuronal nets in the insular cortex. Alcohol. Clin. Exp. Res. 39, 1930–1938.

Deak, A., Bacskai, T., Gaal, B., Racz, E., Matesz, K., 2012. Effect of unilateral labyrinthectomy on the molecular composition of perineuronal nets in the lateral vestibular nucleus of the rat. Neurosci. Lett. 513, 1–5.

Dityatev, A., Schachner, M., 2003. Extracellular matrix molecules and synaptic plasticity. Nat. Rev. Neurosci. 4, 456–468.

Fawcett, J., 2009. Molecular control of brain plasticity and repair. Prog. Brain Res. 175, 501–509.

Foscarin, S., Ponchione, D., Pajaj, E., Leto, K., Gawlak, M., Wilczynski, G.M., Rossi, F., Carulli, D., 2011. Experience-dependent plasticity and modulation of growth regulatory molecules at central synapses. PLoS One 6, e16666.

Galtrey, C.M., Asher, R.A., Nothias, F., Fawcett, J.W., 2007. Promoting plasticity in the spinal cord with chondroitinase improves functional recovery after peripheral nerve repair. Brain J. Neurol. 130, 926–939.

Gogolla, N., Caroni, P., Luthi, A., Herry, C., 2009. Perineuronal nets protect fear memories from erasure. Science 325, 1258–1261.

Happel, M.F., Niekisch, H., Castiblanco Rivera, L.L., Ohl, F.W., Deliano, M., Frischknecht, R., 2014. Enhanced cognitive flexibility in reversal learning induced by removal of the extracellular matrix in auditory cortex. Proc. Natl. Acad. Sci. U. S. A. 111, 2800–2805.

Hartig, W., Brauer, K., Bruckner, G., 1992. Wisteria floribunda agglutinin-labelled nets surround parvalbumin-containing neurons. Neuroreport 3, 869–872.

Kecskes, S., Gaal, B., Racz, E., Birinyi, A., Hunyadi, A., Matesz, C., 2015. Extracellular matrix molecules exhibit unique expression pattern in the climbing fiber-generating precerebellar nucleus, the inferior olive. Neuroscience 284, 412–421.

Mauney, S.A., Athanas, K.M., Pantazopoulos, H., Shaskan, N., Passeri, E., Berretta, S., Woo, T.-U.W., 2013. Developmental pattern of perineuronal nets in the human prefrontal cortex and their deficit in schizophrenia. Biol. Psychiatry 74, 427–435.

McRae, P.A., Porter, B.E., 2012. The perineuronal net component of the extracellular matrix in plasticity and epilepsy. Neurochem. Int. 61, 963–972.

Mulligan, K.A., van Brederode, J.F., Hendrickson, A.E., 1989. The lectin Vicia Villosa labels a distinct subset of GABAergic cells in macaque visual cortex. Vis. Neurosci. 2, 63–72.

Paxinos, G, Watson, C., 2007. The Rat Brain in Stereotaxic Coordinates: Hard Cover Edition. Elsevier Science.

Pizzorusso, T., Medini, P., Berardi, N., Chierzi, S., Fawcett, J.W., Maffei, L., 2002. Reactivation of ocular dominance plasticity in the adult visual cortex. Science 298, 1248–1251.

Racz, E., Gaal, B., Kecskes, S., Matesz, C., 2014. Molecular composition of extracellular matrix in the vestibular nuclei of the rat. Brain Struct. Funct. 219, 1385–1403.

Slaker, M., Churchill, L., Todd, R.P., Blacktop, J.M., Zuloaga, D.G., Raber, J., Darling, R.A., Brown, T.E., Sorg, B.A., 2015. Removal of perineuronal nets in the medial prefrontal cortex impairs the acquisition and reconsolidation of a cocaine-induced conditioned place preference memory. J. Neurosci. Off. J. Soc. Neurosci. 35, 4190–4202.

Soleman, S., Filippov, M.A., Dityatev, A., Fawcett, J.W., 2013. Targeting the neural extracellular matrix in neurological disorders. Neuroscience 253, 194–213.

Sternberg, S.R., 1983. Biomedical image-processing. Computer 16, 22–34.

Suttkus, A., Morawski, M., Arendt, T., 2016. Protective properties of neural extracellular matrix. Mol. Neurobiol. 53, 73–82.

Vazquez-Sanroman, D., Carbo-Gas, M., Leto, K., Cerezo-Garcia, M., Gil-Miravet, I., Sanchis-Segura, C., Carulli, D., Rossi, F., Miquel, M., 2015a. Cocaine-induced plasticity in the cerebellum of sensitised mice. Psychopharmacology 232, 4455–4467.

Vazquez-Sanroman, D., Leto, K., Cerezo-Garcia, M., Carbo-Gas, M., Sanchis-Segura, C., Carulli, D., Rossi, F., Miquel, M., 2015b. The cerebellum on cocaine: plasticity and metaplasticity. Addict. Biol. 20, 941–955.

Wang, D., Fawcett, J., 2012. The perineuronal net and the control of CNS plasticity. Cell Tissue Res. 349, 147–160.

Wang, D., Ichiyama, R.M., Zhao, R., Andrews, M.R., Fawcett, J.W., 2011. Chondroitinase combined with rehabilitation promotes recovery of forelimb function in rats with chronic spinal cord injury. J. Neurosci. Off. J. Soc. Neurosci. 31, 9332–9344.

Xue, Y.-X., Xue, L.-F., Liu, J.-F., He, J., Deng, J.-H., Sun, S.-C., Han, H.-B., Luo, Y.-X., Xu, L.-Z., Wu, P., 2014. Depletion of perineuronal nets in the amygdala to enhance the erasure of drug memories. J. Neurosci. 34, 6647–6658.

Yamada, J., Jinno, S., 2013. Spatio-temporal differences in perineuronal net expression in the mouse hippocampus, with reference to parvalbumin. Neuroscience 253, 368–379.

Yang, S., Cacquevel, M., Saksida, L.M., Bussey, T.J., Schneider, B.L., Aebischer, P., Melani, R., Pizzorusso, T., Fawcett, J.W., Spillantini, M.G., 2015. Perineuronal net digestion with chondroitinase restores memory in mice with tau pathology. Exp. Neurol. 265, 48–58.

Yutsudo, N., Kitagawa, H., 2015. Involvement of chondroitin 6-sulfation in temporal lobe epilepsy. Exp. Neurol. 274, 126–133.